ISSN 2321-807X
Volume 12 Number12
Journal of Advances in chemistry

Batch and column studies on methylene blue using activated carbon/Al_2O_3 nano-composite and its impregnated calcium alginate beads

Ushadevi Balasubramani, Sangeetha Subramaniam, Liviu Mitu, Vairam Sundararajan*
Department of Chemistry, Government College of Technology, Coimbatore, India-641013
busharaman@gmail.com
Department of Chemistry, Government College of Technology, Coimbatore, India-641013
ssgcbe@yahoo.co.in
Department of Chemistry, University of Pitesti, Pitesti, Romania.
Liviu.mitu@upit.ro
Department of Chemistry, Government College of Technology, Coimbatore, India-641013
vamshen@yahoo.com

ABSTRACT

Activated carbon/Al_2O_3 nano-composite (ANC) was synthesized by simple pyrolysis after incorporating the aluminium acetate precursor in activated carbon (AC) matrix. The as-synthesized composite was characterized by FT-IR, XRD, BET isotherm, SEM, EDX, and TEM. The size of Al_2O_3 nanoparticles in carbon matrix was found to be in the range of 10-35 nm. Adsorption characteristics of nano-composite was evaluated using methylene blue dye (MB) by batch and column studies. In batch process, the effect of concentration, temperature and pH were investigated. Batch adsorption study was interpreted with Langmuir, Freundlich, Temkin and Dubinin-Radushkevich (D-R) isotherms. Results showed that adsorption follows Freudlich isotherm model with an adsorption capacity of 116 mg/g at pH 7 at 30 °C and it increases with increase in pH. Kinetic data indicated that the adsorption of dye follows pseudo-second order kinetics model. The negative value of ΔG indicates the spontaneous nature of the adsorption process. For column study the nano-composite was fabricated into Calcium alginate beads (CAB). The performance of CAB was studied with different influent concentrations of MB, pH and bed depth and the results have been interpreted using Thomas and BDST models. The column shows an adsorption capacity of 285.57 mg/g of CAB at pH 7 with bed height of 10 cm and best fitted to BDST model. These outcomes indicate the capability of carbon/Al_2O_3 nano-composite for dye removal.

Keywords: Nano-composite, Adsorption Isotherms, Adsorption kinetics, Calcium alginate, Fixed-bed Column, methylene blue.

1.INTRODUCTION

Environmental pollution is one of the serious global concerns, with a rapid upsurge of industrialization. The waste products engendered from industries such as textile, chemical, food, cosmetics, leather and metallurgical are major sources of soil and water contamination [1, 2].Dyes are common contaminants originating predominantly from textile industries, consequently the removal of dyes from industrial effluents is one of the environmental issues today. Numerous techniques are being employed for achieving removal of dyes from wastewater. Of all the techniques, adsorption has evolved as one of the successful physical method for purification of the textile wastewater, since it is economical and produces high-quality water. Many adsorbents are available such as activated carbon, Bentonite, Sepiolite, Zeolite, Kaolin [3] etc., while activated carbon shows good adsorption towards non-polar pollutants and dyes because of large surface area and microporous nature. Owing to the distressing challenges in the demand for unpolluted drinking water, researchers have been intensely involving in the development of new materials and methods for water purification.

In recent years, nano-adsorbents are designed for the effective removal of toxic contaminants from the environment within a reasonable cost. The development of novel nano-material with good efficacy, capacity and selectivity for heavy metals, dyes and other contaminants is an evolving area of research. The advantages of using nano-adsorbents are mainly attributed to their large surface area and high reactivity. These adsorbents can be used to remove the water contaminants effectively. Various types of nano-materials have been developed, each having distinctive potential to remove the industrial pollutants. Amongvariousnano-materials oxide-based nano-adsorbents such as Fe_3O_4, TiO_2, Mn_3O_4 and their composites [4] play a vital role. The magnetic quality of nanocomposites such as Fe_3O_4, Mn_3O_4, helps for removal and recovery of metal ions and dyes from waste water. These composites can be reused after magnetic separation by removing adsorbed contaminants [5, 6, 7]. In addition, their surface modification by incorporating into inorganic shells improves the uptake of specific pollutants sites and thus enhances the efficacy of the adsorbents.

Alumina (Al_2O_3) has been used to adsorb metals, organic compounds, phenols, gases and dyes [8, 9, 10] etc. It has also been reported that alumina nanoparticles [11] and spinel magnesium aluminate nanoparticles [12] were applied for the adsorption of methylene blue. Activated carbon- alumina composite prepared by in-situ synthesis using aluminium nitrate and aqueous ammonia solution, has been used for adsorption of methylene blue from water [13].

In the present work, methylene blue (MB) was selected as a model for assessing the capability of the synthesized nano-composite. Methylene blue is basic, water soluble dye and is broadly used as coloring agent. It is found to cause several effects such as increased heart rate, cyanosis, vomiting, and on inhalation it leads to breathing difficulty, while

consumption through mouth it causes a burning sensation, nausea, vomiting, diarrhea and gastritis [14]. The adsorption capacities by various commercial carbon and coal, activated carbons derived from agricultural and industrial wastes and biosorbents towards methylene blue have been reported [15].

The sorption capacity parameter obtained from a batch study is useful in understanding the effectiveness of the adsorbent for a specific adsorbate. However, the data are generally not applicable for industrial treatment methods which involve continuous flow fixed bed columns. But the main drawback is that the contact time is not adequately long for the attainment of equilibrium. Moreover, the column packing of nano-materials is still a problem until they are immobilized in a suitable substrate.

Alginate beads are commonly used in immobilization of enzymes and living cells [16]. It is also widely used in immobilization of activated carbon, carbon nano tubes, titania, and magnetite [17]. Biosorptionof metals [18], organic dye [19] by calcium alginate beadshas been reported. Also removal of organic dyes [20, 21, 22] and metals [23] from aqueous solution by composite incorporated calcium alginate beads was investigated. Alginate, a biopolymer extracted from brown algae, is versatile and cheap. The carboxylate groups on the polymer give it the ability to undergo a sol-gel transition with calcium ions to form beads.In order to overcome the difficulty, the composite was immobilized by encapsulating in calcium alginate biopolymer and used in the column study.

To our knowledge, no column study on nano-composite encapsulated alginate beads for the removal of dye, with the study of column performance using kinetic and BDST models has been reported. Therefore the objectives of the study were as follows, to synthesize carbon/alumina nano-composite, to evaluate the effectiveness of the new synthesized composite as adsorbent for the removal of methylene blue dye by batch process and finally to investigate the applicability of carbon/Al_2O_3 immobilized in calcium alginate by column method.

2. MATERIALS AND METHOD

The materials used in this study are methylene blue (BDH), activated carbon (SDFCL), aluminium acetate (SDFCL),sodium alginate (SDFCL), calcium chloride (Fischer), 1:1 hydrochloric acid (38%) and sodium hydroxide.

2.1. Adsorbent

The composites were prepared by mixing a metal carboxylate (aluminium mono basic acetate, 7.6 g) and activated carbon (AC, 10 g) with 50 ml of water and stirred constantly for four hours. The slurry was then dried and heated in a closed furnace without allowing much oxygen at 400°C for 2h and theyield of the carbon/alumina nano-composite(ANC) was 58%.

For column study, the nano-composite was fabricated into beads using Ca-alginate. A weighed quantity of 0.5g of composite was stirred with 2% aqueous solution of sodium alginatefor 30 minutes to form homogeneous solution, and extruded into 10% calcium chloride solution to form beads. The fabricated beads were kept in $CaCl_2$ solution for minimum of 6 h for hardening, washed several times with distilled water to remove excess unbound $CaCl_2$ and packed in the column.

2.2. Characterization of Adsorbent

2.2.1. Characterization of ANC

The synthesized composite ANC was characterized by IR (SHIMADZU-IR PRESTIGE 21), XRD (SHIMADZU XRD 6000), SEM (JOEL JFM 6390), EDX (OXFORD INSTRUMENT), DLS, BET isotherm study (QUANTACHROME NOVA 1200E-Surface area and Poreanalyser) and HR TEM (JEOL/JEM 2100).The absorbance of MB dye was recorded using UV-Visible spectrophotometer (HACH- DR 5000).

2.2.2. Characterization of CAB

The beads are found to be spherical and black in color, due to presence of carbon nano-compoiste. The beads extruded are uniform with size of 34 mm diameter weighing 28±2 mg and shows good reproducibility. The structural morphology of CAB was visualized by FESEM(ZEISS Sigma VP FEG SEM), by using cross-sectioned dry beads. The composition of the beads was determined by EDAX before and after adsorption of MB dye.

2.3. Batch studies

A stock solution of 1000 mg/L were prepared using double distilled water and all the working solutions were prepared by diluting the stock solution. The dye adsorption measurements for batch studies were studied for concentration range of 5 to 40 mg/L. The dye solutions of 50 ml portions were stirred with 0.01 g of the adsorbent for 1 hour. The effect of pH variation was studied at pH varying from 1-14 taking 50 ml of 25mg/L solution with 0.01g of adsorbent.

2.4.Column studies

Continuous flow adsorption studies were conducted in a glass column (1.5 cm internal diameter and 30 cm height). A series of experiments was conducted with various influent concentration, and pHtaking the mass of adsorbent beads in the column, 8.8 g at pH 7. The effect of bed depth on adsorption was carried out by taking three different bed depths, viz., 10 cm (8.8 g), 12 cm (10.6 g), 15 cm (13.4 g), and MB concentration of 25mg/L at a flow rate of 2.5 ml/min. The effect of concentration and pH was studied at three different concentrations viz 15, 25, and 50mg/L and at pH 3, 7

and 12, by adding HCl or NaOH solution. The MB solution was pumped to the column in a down flow direction by a peristaltic pump at 2.5 ml min^{-1}.The residual methylene blue concentration of each study was determined by using UV/Visible spectrophotometer at the wavelength of maximum absorbance (670 nm).

2.5.Models applied

In batch study adsorption behaviour of the composite (ANC) is evaluated by isotherm studies, Langmuir, Freundlich, Temkin, Dubinin-Radushkevichwere fitted to predict the best fit model. The amount of MB adsorbed onto ANC was calculated using the following equation,

$$q_e = \frac{(C_o - C_e)V}{W} \qquad (1)$$

where C_o and C_e are the initial and equilibrium concentration (mg/L) repectively, V, volume of the dye solution (L), w, weight of the adsorbent used (g) and q_e, amount of MB adsorbed at equilibrium.

For column studies, Thomas and BDST models were used to predict the performance of the adsorbent encapsulated in alginate beads. The error analysis parameters of different kinetic models in column study were obtained using linear analysis according to least square of errors. The relative mathematical formula is,

$$SS = \sum \frac{(y_e - y_c)^2}{N} \qquad (2)$$

Where y_e and y_c are the experimental value and calculated value respectively according to the model, and N is the number of the experimental points.

3. RESULTS AND DISCUSSION

3.1.Characterization of adsorbent

3.1.1. IR Analysis

FT IR spectra of AC, AC incorporated aluminium acetate (ACAA), composite (ANC), MB adsorbed composite (MB-ANC) are shown in Fig.1 a to d. All the spectra exhibit common absorption bands around 3600 cm^{-1} (u_{O-H}), 3400cm^{-1}(u_{N-H}) , 2800 cm^{-1} ($u_{C-H\ alkyl}$), 1100 cm^{-1} (u_{C-C}) implying the presence of –O-H, -N-H, -C-H, -C-C groups in the AC. The presence of the peaks at 1520 to 1580 cm-1($u_{C=O}$ asymmetric) and 1380 to 1460 cm-1 ($u_{C=O}$ symmetric) in the spectra of ACAA (Fig. 1 b) indicates that the metal carboxylate is incorporated in activated carbon. These peaks are found to be absent in the composites substantiating the destruction of metal carboxlates to metal oxide in carbon matrix. This fact is further confirmed by display of peaks around 470- 524 cm^{-1} and 690 cm^{-1}(u_{Al-O}) (Fig. 1 c). Comparing the spectra of ANC with that of methylene blue adsorbed composite (MB-ANC) it is observed that the absorption peaks characteristics of methylene blue, 1600 $cm^{-1}$to 1580 cm^{-1} ($u_{C=C-C\ in\ ring}$) and 1500 cm^{-1} to 1400 cm^{-1} ($u_{C-C\ aromatic\ ring}$) (Fig.1 d) are found in the spectra of MB-ANC. This is further corroborated by the shifts of -NH peaks from around 3440 cm^{-1} in composites to 3400 cm^{-1} in MB adsorbed composites.

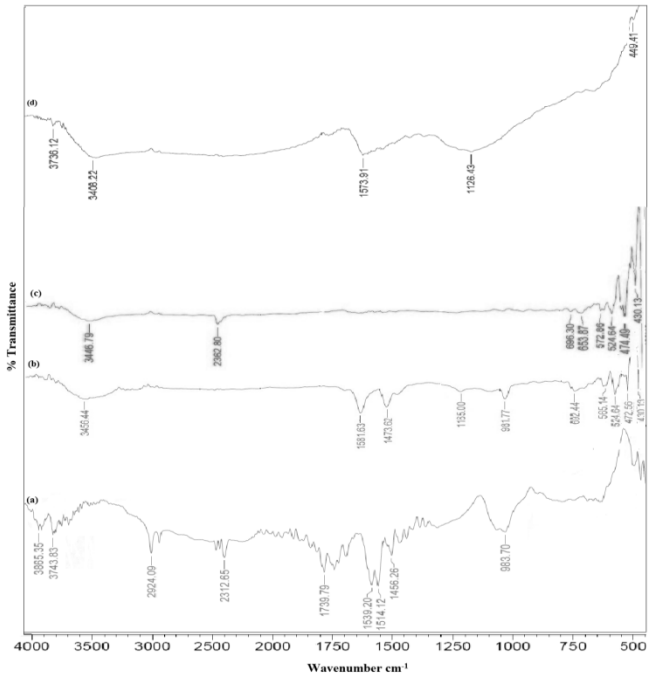

Fig. 1 IR spectra of AC (a), ACAA (b), ANC (c), MB-ANC (d)

3.1.2. XRD Analysis

The XRD patterns of AC and ANC are shown in Fig.2 (a, b respectively). In this study 2θ value at 26.6˚ corresponding to carbon (JCPDS card no. 26-1080) found in Fig.2 a, are also observed in Figure 2 (b) and this fact confirms the presence of carbon in nano composites. Insertion of Al_2O_3 in AC was confirmed by the patterns agreeing well with JCPDS card no. 10-0173. The peaks indexed at 35.09˚ (104), 41.06˚ (006), 43.88˚ (113), 52.91˚ (024), 57.79˚ (116), 59.90 ˚ (211), 66.84 ˚ (241), 70.35 (125) and 77.47˚ (119) in Fig 2 b match well with Alumina (JCPDS card No 10-0173) structure. Applying FWHM values in Scherrer'sformula, D=kλ/βcosθ, where λ is x-ray wavelength (0.154nm), β, FWHM of a diffraction peak, θ, diffraction angle and k,Scherrer's constant of the order of 0.89, it is calculated that the average crystallite size of metal oxides is in the range of 10-40nm

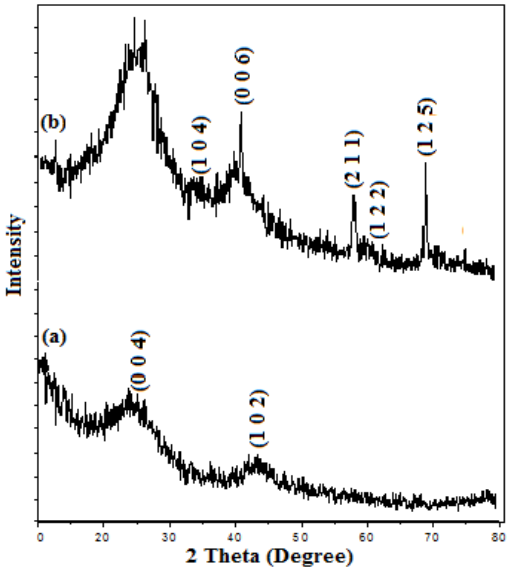

Fig.2 XRD image of AC (a) and ANC (b)

3.1.3. SEM Analysis

The SEM and EDX images of ANC before MB adsorption and after MB adsorption was shown in Fig.3. The atomic ratio of oxygen to metal shown by the EDX of composite also substantiates that metal oxide (Al_2O_3) are inserted into carbon (Fig. 3 b). The adsorption of MB onto the synthesized ANC was also evidenced by the SEM and EDX images of ANC after MB adsorption (Fig. 3 c & b), EDX image shows the presence of peaks for nitrogen and sulphur .

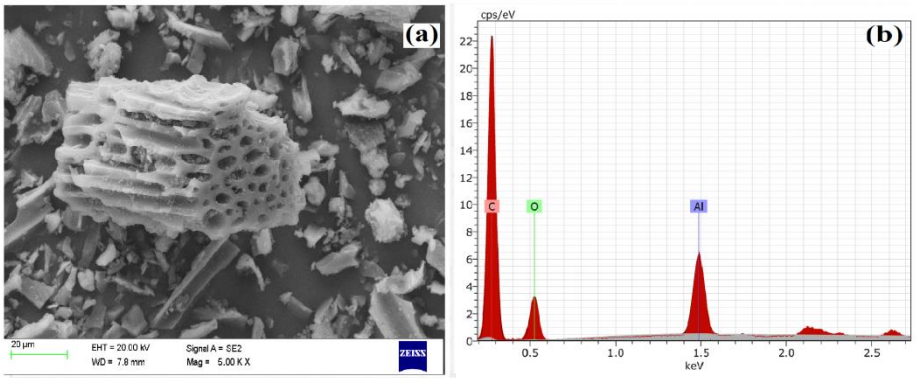

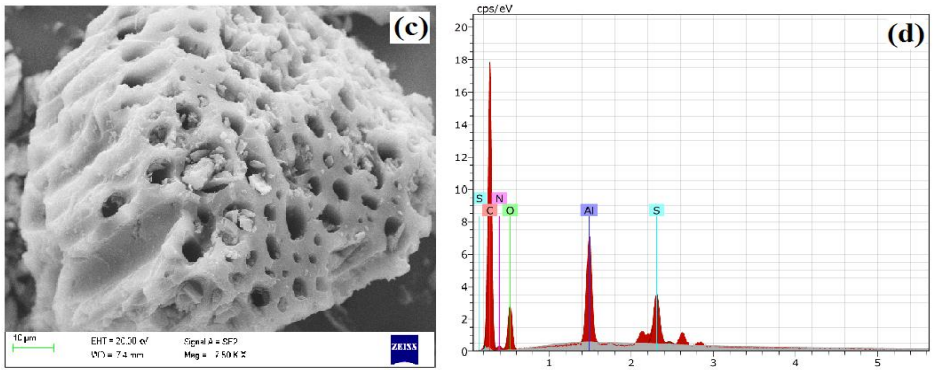

Fig.3 SEM and EDX images of ANC before MB adsorption (a, b) and after MB adsorption (c, d)

3.1.4. TEM Analysis

TEM images shown in Fig.4 light shade region is AC and dark spherical shape region is nanoparticles. From Figure 5, the size of nanocomposites is observed in the range of 10 – 40 nm, which agrees well with the results obtained in XRD.

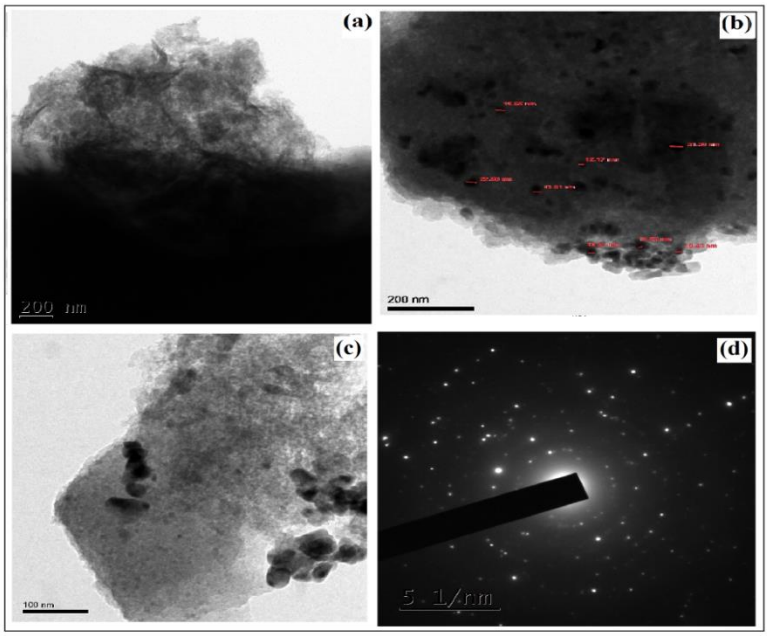

Fig.4 TEM images of ANC (a, b, c) & and SAED pattern (d)

3.1.5. BET Analysis

Nitrogen adsorption-desorption curve was shown in Fig.5.The measurements were conducted to evaluate the pore sizes, pore volume and the Brunauer-Emmett-Teller (BET) surface area of the composite. The composite have pore size, pore volume and BET surface area of 6.023 nm, 0.99 cc/g and 342.08 m^2 g^{-1} respectively.

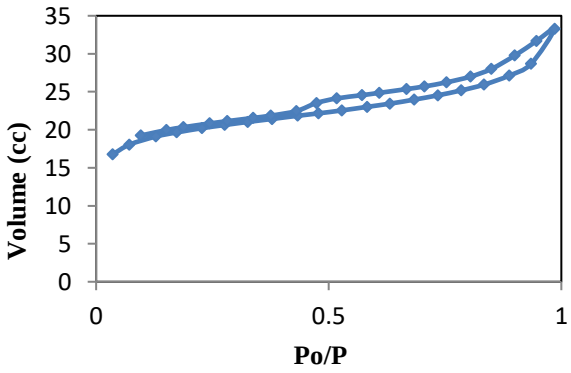

Fig.5 Nitrogen adsorption and desorption curve for ANC

3.2. Batch adsorption study

3.2.1. Adsorption Isotherm study

Langmuir, Freundlich, Temkin and Dubinin-Radushkevich equations [24] were used to suggest the adsorption isotherms at 303, 313, and 323K.

The Langmuir adsorption model is based on the assumptions that adsorption follows unilayer and there is no lateral interaction between the adsorbed molecules on the surface. The linear form of Langmuir equation is represented as,

$$\frac{1}{q_e} = \frac{1}{q_m} + \frac{1}{bq_m c_e} \qquad (3)$$

where c_e (mg/L) is the equilibrium concentration of MB in solution, q_e(mg/g), maximum amount of MB adsorbed at equilibrium, q_m (mg/g), maximum amount of MB adsorbed per unit mass of adsorbent required for monolayer coverage of the surface and b (L/mg) is the Langmuir constant. The slope and the intercept of linear plots of $1/c_e$against $1/q_e$ (Fig.6a) yield the values of $1/bq_m$ and $1/q_m$for equation (3). The values of b, q_m, and R^2 calculated from the linear forms are given in Table 1.

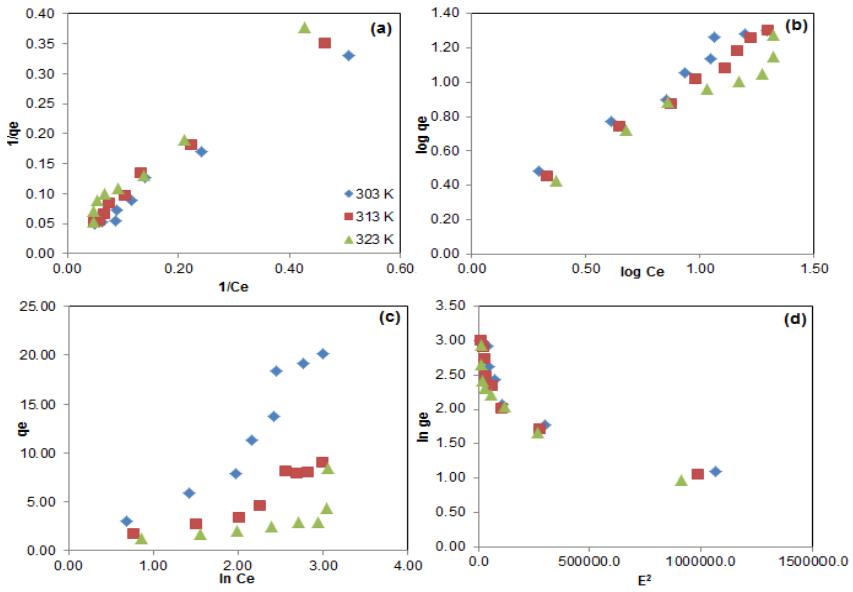

Fig. 6 Adsorption isotherms of ANC at 303 K, 313 K, 323 K Langmuir (a), Freundlich (b), Temkin (c), D-R Isotherm (d)

The Freundlich isotherm model can be used for non-ideal multilayer sorption on heterogeneous surfaces. The linear form of Freundlich isotherm model can be expressed as,

$$\log q_e = \log K_F + 1/n \log c_e \qquad (4)$$

where K_F is the Freundlich constant indicative of adsorption capacity of the adsorbent, and n is another constant related to the surface homogeneity. Using the slope and intercept of linear plots of log q_e against log c_e (Fig.6b), the values of 1/n and log K_F obtained,are given in Table 1. The Freundlich constant, n, in the range of 1 to 10 is considered for classification as favourable adsorption. The n values at various temperatures observed here 1.14, 1.15, 1.34 shows that adsorption capacity by Freundlich isotherm is favourable.

Table 1: Adsorption constants for adsorption of MB onto ANC

	Isotherm constants												
T (K)	**Langmuir**			**Freundlich**			**Temkin**			**DR constants**			
	q_m	b	R^2	K_F	n	R^2	A	B	R^2	q_s	K_{ad}	E	R^2
303	59.89	0.027	0.947	1.67	1.14	0.9648	1.77	8.14	0.8877	14.93	$2x10^{-6}$	0.5	0.9455
313	46.73	0.029	0.901	1.43	1.15	0.9901	1.86	3.58	0.8680	13.62	$2x10^{-6}$	0.5	0.8839
323	30.88	0.041	0.845	1.53	1.34	0.9436	2.01	1.98	0.4708	11.79	$2x10^{-6}$	0.5	0.8286

Temkin model considered the effects of interaction between the adsorbate and the adsorbent. The linear form of Temkin isotherm equation can be expressed as,

$$q_e = B \ln A + B \ln c_e \quad (5)$$

where B = RT/b, T is the absolute temperature (K), R is the universal gas constant (8.314 J/mol/K), A is the equilibrium binding constant (L/mg) and B is related to the heat of adsorption. The linear plot of q_e against $\ln c_e$ at various temperatures are presented in Fig.6c. Temkin constants A, B, and R^2 values are given in Table 1. Dubinin and Radushkevich model relates the characteristic adsorption curve with the porosity of the sorbent. The linear form of D-R isotherm equation is,

$$\ln (q_e) = \ln (q_s) - \beta \varepsilon^2 \quad (6)$$

where$q_e$is the amount of absorbate adsorbed per unit dosage of adsorbent (mg/g),q_s, the theoretical isotherm saturation capacity (mg/g), β, DubininRadushkevich isotherm constant(mol^2/J^2), ε, Dubinin isotherm constant. The value of ε can be calculated as,

$$\varepsilon = RT \ln (1+1/ c_e) \quad (7)$$

where R, T and c_e represents the gas constant (8.314 J/mol/K), absolute temperature (K), and adsorbate equilibrium concentration (mg/L) respectively. The linear plot of ln q_e against ε^2 (Fig.6d) yields the value of q_m and β. The value of mean adsorption energy E (KJ/mol), was calculated using D-R parameter β in the equation,

$$E=1/\sqrt{2\beta} \quad (8)$$

The value of mean adsorption energy gives information about chemical and physical adsorption. The mean adsorption energy (E) the adsorbent at temperatures 303, 313 and 323 K is lesser than 8 kJ/mol which indicates that the adsorption of MB follows essentially physisorption [25]. From Table.1, the low correlation coefficient value denotes that the adsorption doesn't follows Langmuir isotherm, indicating that the adsorption was not monolayer. The determined coefficient R^2 suggests that the adsorption follows predominantly Freundlich isotherm model.

3.2.2 Mechanism of adsorption

Methylene blue is a heterocyclic cationic dye (Fig.7) which has special affinity for negatively charged surfaces and commonly undergoes chemical adsorption.

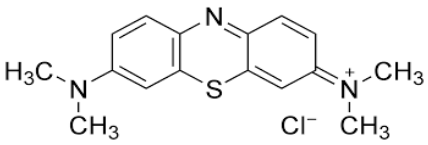

Fig.7.Structure of Methylene blue

The dye molecule may be adsorbed on specific sites instead of the total surface areas, monomeric or dimeric aggregates [26]. The equilibrium reactions of MB molecules [27] in aqueous medium are,

$$(MB)_2 \rightleftharpoons 2\ MB \quad (9)$$

$$MB + H_2O_{ad} \rightleftharpoons MB_{ad} + H_2O \quad (10)$$

$$(MB)_2 + H_2O_{ad} \rightleftharpoons (MB)_{2ad} + H_2O \quad (11)$$

$$(MB)_2 + 2\ H_2O_{ad} \rightleftharpoons 2\ MB_{ad} + 2\ H_2O \quad (12)$$

Al_2O_3 inside the carbon matrix formtheir hydroxides on the surface of particles in aqueous medium. The affinity between -OH groups in the composites and the $-N(CH_3)_2$ groups in the Methylene blue molecule will be high.

Being monofunctional in a polar solvent MB follows S and L type curves [28] predominantly on a polar composite substrate. This shows that orientation of MB molecule on the adsorbent surface occurs with strong intermolecular attraction. The association of MB molecule with the adsorbent ANC involves hydrogen bonding and van der waals forces of -OH and $-N(CH_3)_2$ groups. Thus chemisorption accompanied with physisorptionoccurs in the adsorption of MB onto the ANC.

3.2.3. Effect of pH

The effect of pH variation was studied at pH varying from 1- 12 of 50 ml of 25mg/L solution with 0.01g of adsorbent. A plot of percentage removal with pH variation is shown in Fig.8. The alumina present in the nano-composite when dispersed in water forms Al–OH kind of groups. In acidic medium, Al^{3+} ions are formed causing increase in the total positive charge of the particle as given in equation (15) [29],

$$Al(OH)_2^+ + OH^- \rightleftharpoons Al^{3+} + 3\ OH^- \quad (13)$$

At alkaline pH, $Al(OH)_3$ acts as an acid due to the presence of excess of OH^- ions as shown in equation (16),

$$Al(OH)_3 \rightleftharpoons Al(OH)_2\ O^- + H^+ \quad (14)$$

This leads to the formation of the negative charge on the particles. At neutral pH, $Al(OH)_3$ molecules are ionised as given in equation (17), the hydroxide formed acts as a base due to the presence of excess of H^+ ions, and suppresses acid ionisation.

$$Al(OH)_3 \rightleftharpoons Al(OH)_2^+ + OH^- \quad (15)$$

As a result, the potential determining ion is $Al(OH)_2^+$ and the particle surface is positively charged. Owing to the above facts, the adsorption of MB dye on Al_2O_3 should decrease in neutral and acidic pH conditions and increase in alkaline pH condition. This has been observed in the experiments also, ie adsorption increases with pH and reaches saturation after pH 10.

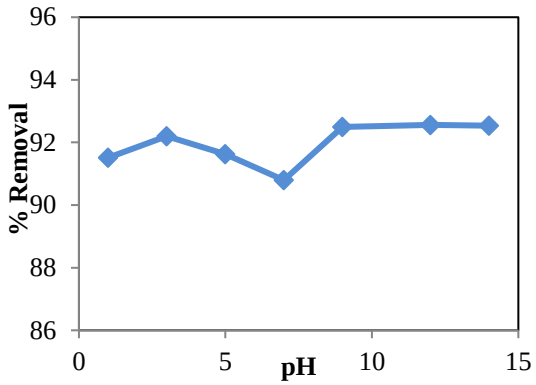

Fig.8. Effect of pH

3.2.4.Adsorption kinetics

3.2.4.1. Pseudo first order and Pseudo second order kinetics

A comparison of pseudo first order and pseudo second order kinetic studies of adsorption of MB dye by the adsorbent ANC is shown in Fig. 9 a & b. The kinetic equations [25] used are:

Pseudo-first order kinetic equation: $\log (q_e - q_t) = \log q_e - k_1 t/2.303$ (16)

Pseudo-second order kinetic equation: $t/q_t = 1/k_2 q_e^2 + t/q_t$ (17)

whereq_e and q_t are the amounts of MB adsorbed at equilibrium and at time t (min), t is the adsorption time(min), and k_1 (min^{-1}) and k_2 (g $mg^{-1}min^{-1}$) are pseudo-firstorder and pseudo-second order rate constants, respectively. The kinetic constants obtained by linear regression for the two models are summarized in Table 2. The correlation coefficients R^2 values for pseudo-second order model are found to be closer to unity and the calculated q_e values agree well with the experimental values

Table 2: Rate constants for Pseudo-first order, Pseudo-second order kinetic and Intra-particle Diffusion models

Pseudo-first order			Pseudo-second order			q_{eexp}	Intraparticle Diffusion model		
k_1	q_e	R^2	k_2	q_e	R^2		K_{int}	I	R^2
0.0191	2.60	0.9643	0.0391	22.60	0.9997	23.18	2.6065	5.90	0.7068

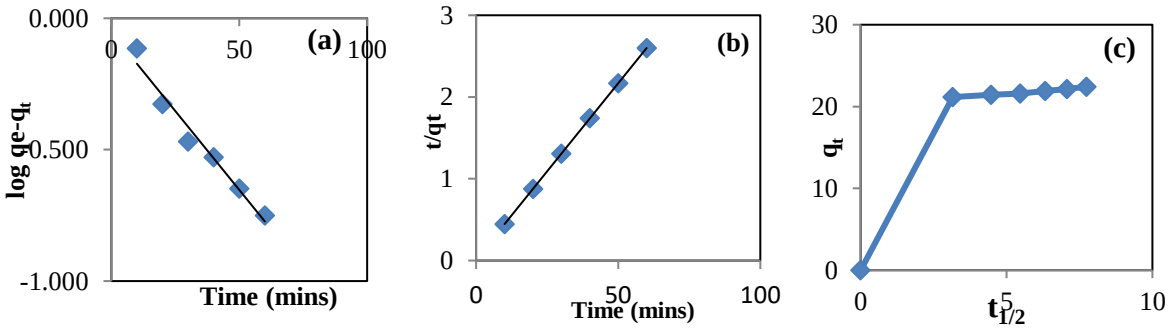

Fig. 9 Kinetic models- Pseudo-first order (a), Pseudo-second order (b) and Intra-particle diffusion model (c)

3.2.4.2.Intra-particle Diffusion

Kinetic data were further analysed using intra-particle diffusion approach proposed by Webber and Morris [30]. It can be used to predict whether intra-particle diffusion is the rate-limiting step. According to this theory, the intra-particle diffusion model can be expressed as,

$$q_t = K_{int}\, t_{1/2} + I \qquad (18)$$

where q_t is the amount of MB adsorbed at time (t), K_{int}, intra-particle diffusion rate constant(mg/g $min^{1/2}$), I, intercept (mg/g), Fig. 9c shows the plot of q_t against $t_{1/2}$ at 303 K. According to this model there are three portions, initial curve portion due to the immediate utilization of the available sites on the adsorbent surface the linear portionattributed to very slow diffusion of the adsorbate from the surface site into the inner pores and the plateau to equilibrium. For adsorption of MB onto the composites, the plot shows only two portions, a linear portion and then a plateau indicating two stages of adsorption process. The values of K_{int} and I obtained from linear portion are given in Table.2. The R^2 valueis 0.7068, suggesting that intra-particle diffusion model does not fit the experimental data.

3.2.5. Thermodynamic data

The thermodynamic parameters such as entropy change (ΔH°), entropy change (ΔS°) and Gibbs free energy change (ΔG°) were determined by equations (19) and (20)

$$\Delta G = -RT \ln K_p \qquad (19)$$

$$\ln k_p = (\Delta S/R) - (\Delta H/RT) \qquad (20)$$

$$\Delta G = \Delta H - T\Delta S \qquad (21)$$

where R is the gas constant, T, temperature, K_p, equilibrium constant, K_p at different temperatures was determined by plotting $\ln(q_e/C_e)$ versus q_e and extrapolating q_e to zero. The values of ΔG at different temperatures are listed in Table 3. The plot of ΔG against Temperature (T) is shown in Fig.10. The values of ΔS and ΔH are obtained from the slope and the intercept are also summarized in Table.3. From the thermodynamic results, the negative value of ΔG indicates that the adsorption of dye on the composite is spontaneous. A positive value of ΔS indicates the affinity of the adsorbents for MB dye. The ΔH value is positive showing that the adsorption is endothermic.

Table 3: Thermodynamic data of the composite

Temperature, K	ΔG, kJ mol^{-1}	ΔH, kJ mol^{-1}	ΔS, J mol^{-1} K^{-1}
303	-1.138		
313	-1.568	1.56	35.3
323	-1.843		

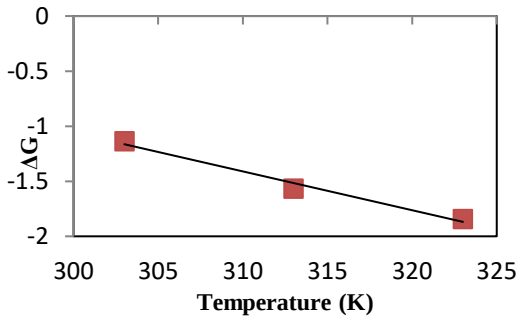

Fig. 10 Van't Hoff plot of MB adsorption

3.3. Column studies

In this work, two models, Thomas and BDST were used to predict the performance of the column.

3.3.1. Thomas model

Thomas model is simple to use and is widely used model in column performance theory. The data obtained in continuous flow column studies is used to calculate the maximum solid phase concentration of adsorbate on adsorbent and the adsorption rate constant using the reaction kinetic model developed by Thomas [31]. The expression for Thomas model for an adsorption column is as follows,

$$\frac{C_t}{C_o} = \frac{1}{1+\exp\left(\frac{K_{Th}\, q_e\, x}{Q} - K_{Th} C_o\, t\right)} \qquad (22)$$

where C_o is the influent MB concentration at time t (mg l^{-1}), C_t the effluent concentration at time t (mg l^{-1}), K_{Th} the Thomas rate constant (mL/min mg), q_e themaximum solid-phaseconcentration of the solute (mg/g), X the mass of adsorbent (g), and Q isthe flow rate (mL/min).The linearized form of the Thomas model is as follows [32],

$$ln\left(\frac{C_o}{C_t}\right) - 1 = \frac{K_{Th}\, q_e\, x}{Q} - K_{Th}\, C_o\, t \qquad (23)$$

The kinetic coefficient K_{Th} and the adsorption capacity of the bed q_e can be determined from a plot of $\ln[(C_0/C_t)-1]$ against$t$ at a given condition. Thomasmodel was applied to the experimental data with regard toinfluent concentration of MB, pH and bed depth. A plot of $\ln[(C_0/C_t)-1]$ against$t$was used to determine the coefficients, and the SS were obtained using linear regression analysis according Eq. (24) and the results were listed in Table 4.

The datas such as Thomas rate constant K_{Th}, adsorption capacity of the bed q_e, regression coefficient R^2, relative constants were obtained using linear regression Thomas model. The R^2 ranges from 0.889 to 0.947 for variance in influent concentration and bed depth studies, showing the correlation of C_0/C_t and t according to equation (22) is significant, but for variance in pH study, the R^2 value ranges from 0.780 to 0.810, showing a slight contrast from this correlation.

3.3.1.1. Effect of concentration

A change in the influent concentration of MB affects the operation characteristics of the fixed bed column. The adsorption breakthrough curves obtained by changing the influent concentration (15, 25 and 50 mg l^{-1}) at 2.5 mL min^{-1}flow rate and 10 cm bed depth are given in Fig.11. Higher influent concentration caused a faster breakthrough and also high uptake of MB molecules leading to more adsorption whereas a lower influent concentration gave delayed breakthrough curve with less adsorption. This is because the lower concentration gradient caused slower transport due to decreased diffusion co-effficient [32]. The values of C_t/C_o reached 0.60, 0.88, and 0.92 when the influent concentration was 50, 25, and 15 mg l^{-1} respectively in the duration of 15 minutes. These results demonstrate that the change of concentration gradient affects the saturation rate and breakthrough time. The diffusion process is concentration dependent [33] i.e., as the influent concentration increases MB diffusion rate increases.

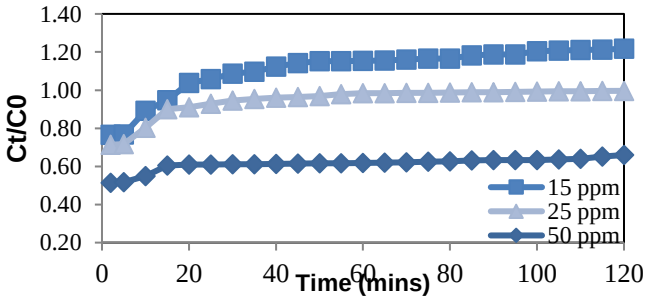

Fig. 11. Breakthrough curve of the effect of concentration on adsorption of MB onto ANC

MB ions being positively charged strongly are adsorbed onto CAB, due to electrostatic interaction with the hydrated alumina encapsulated into the bead and carboxylate functional group present in alginate molecules. The adsorption occurs so fast that the uptake of dye occurs within the first five minutes (nearly 50%) and the breakthrough reaches within 5 minutes. At lower influent concentration, breakthrough occurs very slowly, as the influent concentration increases a sharper breakthrough was observed. The reason may be, at lower concentration, MB preferentially is adsorbed onto the encapsulated adsorbent, whereas at higher concentration, ionic exchange of MB with Ca ions bound to carboxylate sites of alginate is favoured [21] along with adsorption onto the incorporated nano-composite.

Table 4: Parameters of Thomas model using linear regression analysis under different conditions

C_o Mg L^{-1}	pH	Z cm	K_{Th} ml $min^{-1}mg^{-1}$	q_e mg g^{-1}	R^2	SS (x 10^3)
15	7	10	2.33	180.71	0.947	26.58
25	7	10	0.92	285.57	0.922	27.30
50	7	10	0.08	585.93	0.912	26.53
25	7	12	0.06	451.77	0.889	25.58
25	7	15	0.04	497.18	0.803	23.11
25	3	10	0.57	50.73	0.810	23.16
25	12	10	0.24	66.28	0.781	23.56

3.3.1.2. Effect of bed depth

To examine the effect of bed depth, three different bed depths namely, 10, 12, 15 cm at same influent concentration (C_o= 25 mg l^{-1}) and flow rate (Q= 2.5 ml min^{-1}), respectively, were studied. The breakthrough curves at different bed depths are shown in Fig. 12. As the bed depth increases, MB has more time to contact with the adsorbent which results in higher removal of MB. The slope of the breakthrough curve decreased with increase in bed height, and high uptake of MB was observed. SEM image of CAB surface shows pores and the MB ions diffuse into the pores on the CAB surface. The cross sectional view of CAB shows number of capillaries like structures (Fig.13) and the diffused dyes get into these capillaries. The increase in adsorption with bed depth was due to increase in the amount of adsorbent and inturn more surface pores and the increased capillaries are available for adsorption of dye molecules.

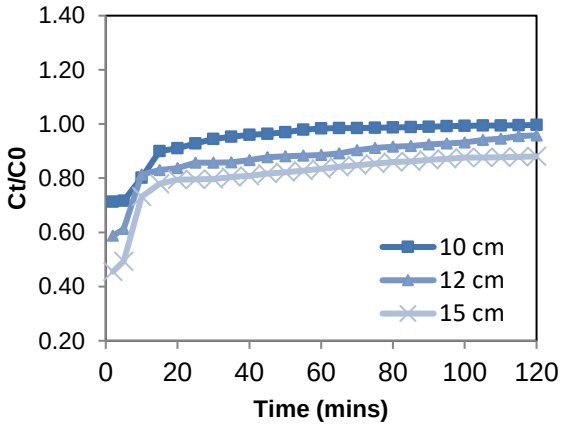

Fig. 12. Breakthrough curve of the effect of bed depth on adsorption of MB onto ANC

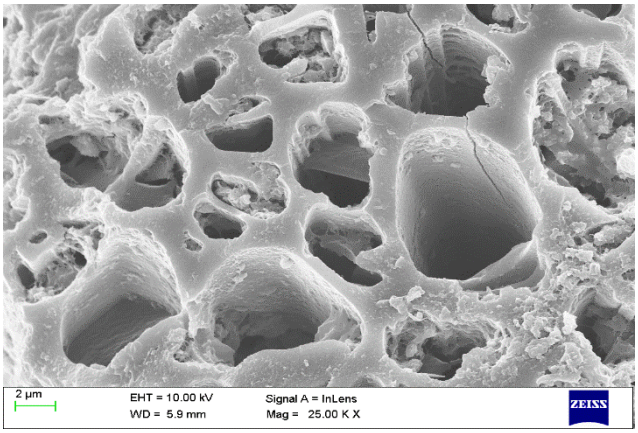

Fig. 13. Cross sectional view of CAB

3.3.1.3. Effect of pH

To inspect the effect of variation in pH, the column adsorption experiments were done at different pH, 3, 7 and 12. A plot of C_t/C_o versus t **(**Fig.14**)** shows the effect of pH on adsorption of MB onto the composite. As the pH was 3 and 12, the value of C_t/C_o was almost same, 0.57 and 0.58 respectively in 20 minutes. But, as the time increases, the removal decreases for pH 3 as the breakthrough curve was 0.67 and C_t/C_o value increases upto0.79. For pH 12, C_t/C_o was not more than 0.66, but at pH 7, the value of C_t/C_o reached 0.81 in 10 minutes. At pH 7 the adsorption of MB ions occurs slowly and at pH 3 the uptake of dye molecules occurs rapidly as it reaches breakthrough by 5 minutes. As the pH of the solution was higher than 10, adsorption increases in batch process, whereas in column study it decreases. Since, at pH 12, the Ca^{2+} ions react with the hydroxyl ions of the solution to form calcium hydroxide, which decreases in cross linking of the beads inturn decrease in adsorption onto the beads. But as soon as the breakthrough point was reached, the adsorption was smoother and a slightly higher than at pH 3.

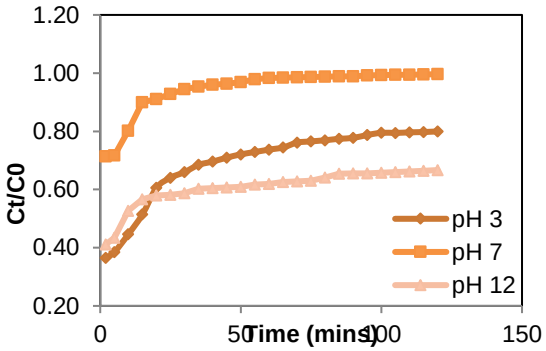

Fig. 14. Breakthrough curve of the effect of pH on adsorption of MB onto ANC

3.3.2 Bed-Depth/Service Time analysis (BDST) model

BDST is a model for predicting the relationship between bed depth, Z and service time, t, in terms of process concentration and adsorption parameters. It is based on the assumption that the rate of adsorption is controlled by the surface reaction between adsorbate and the unused adsorbent capacity [34]. A linear relationship between bed depth and service time is as follows:

$$t = \frac{N_o}{C_o\,F}\,Z - \frac{1}{K_a C_o}\ln\left(\frac{C_o}{C_t} - 1\right) \qquad (24)$$

where t is the service time at breakthrough point (min), N_0 the dynamic bed capacity (mg l^{-1}), Z, the packed-bedcolumn depth (cm), F, the linear flow rate (cm min−1), C_0 and C_t are, the inlet and the breakthrough metal ionconcentrations (mg l^{-1}) respectively,and k_a the adsorption rate constant(l mg^{-1} min^{-1}). The isoremoval lines of t versus Z for C_0/C_t = 0.9, 0.8, 0.7 are shown in Fig. 15.

Table 5: Parameters of BDST model (C_o= 25 mg l^{-1}, Q = 2.5 ml min^{-1})

C_t/C_o	a min cm^{-1}	b min	K_a 1 mg^{-1} min^{-1}	N_o	R^2	SS
0.7	6.05	56.32	0.000463±0.004	734±0.33	0.9924	12.57
0.8	13.28	127.24	0.000435±0.013	469±0.63	0.9656	12.23
0.9	20.78	189.74	0.000601±0.012	214±0.27	0.9944	12.59

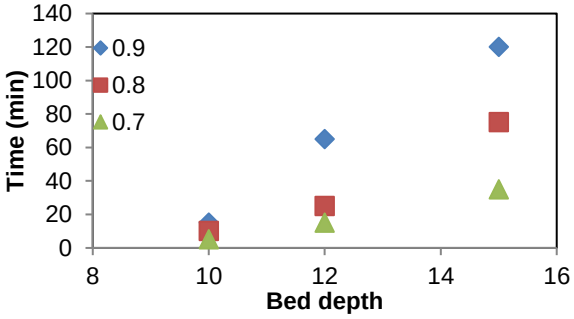

Fig. 15. Isoremoval lines for C_t/C_0 = 0.7, 0.8, 0.9 for different bed height (C_0=25 mg/L, u=2.5 ml/min)

The plot was linear with dermined co-efficient R^2 of 0.994 to 0.965, indicating the validity of BDST for the column under study. The BDST constants obtained from Eq. 25 at flow rate of 2.5 ml min^{-1} and influent concentration 25 mg l^{-1} at C_0/C_t = 0.9, 0.8, 0.7 are listed in Table 5. As the bed depth increases, the residence time of the solution inside the column increases, allowing the MB molecules to diffuse deeper inside the capillaries of CAB. These results indicate that the BDST model gave a good fit for the prediction of adsorption performance of MB onto CAB.

4. CONCLUSION

From the observations made in this work, the following conclusions can be drawn:

- New carbon-alumina nano-composite have been successfully synthesized from aluminium acetate precursor, with alumina reinforcement of 10-35 nm in carbon.
- An adsorption capacity of 116mg /g at pH 7 towards MB dye is acquired by incorporation of alumina particles.

- Increase in pH shows enhanced adsorption due to additional adsorptive effect of hydrated alumina and increase in negative sites on alumina.
- The adsorption study reveals that the adsorption follows Freudlich isotherm and pseudo- second order kinetics. The negative ΔG confirms that the adsorption of MB dye on the adsorbent surface is spontaneous.
- From column studies, it is inferred that BDST model satisfactorily explains the adsorption of MB onto CAB and adsorption increases with concentration. The column adsorption is exceptionally rapid as 50% of MB being adsorbed by CAB within 5 minutes due to cumulative effect of alginate beads.
- Higher the bed depth higher is the removal efficiency of MB, due to the availability of more adsorption sites and also increase in service time. Hence it is suggested that carbon/Al_2O_3 immobilized in calcium alginate beads (CAB) may be applied for dye removal in industrial treatment plants.

Acknowledgements

We wish to acknowledge Sophisticated Analytical Instrument Facility, STIC, Cochin University, Kerala, India for TEM studies and Centre of Excellence, Environmental Science, TEQIP- Phase-II for the financial assistance.

References

[1] Rajkumar, D, and Jong G, K., 2006. Oxidation of various reactive dyes with in situ electro-generated active chlorine for textile dyeing industry wastewater treatment. Journal of Hazardous Materials B136, 203-212. http://dx.doi.org/10.1016/j.jhazmat.2005.11.096

[2] Zakia Sultana, Md. Ershad Ali, Md. SalaUddin, Md. Mominul Haque., 2013. Implementation of Effluent Treatment Plants for Waste Water Treatment. Journal of Environmental Protection, 4, 301-308.http://dx.doi.org/10.4236/jep.2013.43035

[3] Mohamed Amine Zenasni, Bahia Meroufel, André Merlin, Béatrice George., 2014. Adsorption of Congo Red from Aqueous Solution Using CTAB-Kaolin from Bechar Algeria, Journal of Surface Engineered Materials and Advanced Technology. 4, 332-341. http://dx.doi.org/10.4236/jsemat.2014.46037

[4] Sarika Singh, Barick, K, C., Bahadur, D., 2013. Functional Oxide Nanomaterials and Nanocomposites for the Removal of Heavy Metals and Dyes. Nanomaterials and Nanotechnology.3, Art.20, 1- 19

[5] Ranjithkumar, V., Sangeetha, S., Vairam, S., 2014. Synthesis of magnetic activated carbon/α-Fe_2O_3 nanocomposite and its application in the removal of acid yellow 17 dye from water. Journal of Hazardous Materials, 273, 127-135. http://dx.doi.org/10.1016/j.jhazmat.2014.03.034

[6] Mohamed A. Farghali, Taher A. Salah El-Din, Abdullah M. Al-Enizi, Ramadan M. El Bahnasawy., 2015. Graphene/ Magnetite Nanocomposite for Potential Environmental Application. International journal of Electrochemical Science. 10, 529-537.

[7] Yuqian Li, Jiangying Qu, Feng Gao, Siyuan Lv, Lin Shi, Chunxiang He, Jingchang Sun., 2015. In situ fabrication of Mn_3O_4 decorated graphene oxide as a synergistic catalyst for degradation of methylene blue. Applied Catalysis B: Environmental, 162, 268-274.http://dx.doi.org/10.1016/j.apcatb.2014.06.058

[8] Asok Adak., Anjali Pal., Manas Bandyopadhyay., 2006. Removal of phenol from water environment by surfactant-modified alumina through adsolubilization. Colloids and Surfaces A: Physicochemical and Engineering Aspects 277 (1-3), 63-68 http://dx.doi.org/10.1016/j.colsurfa.2005.11.012

[9] Haverkamp, R, G., Metson, J. B, Hyland, M. M, Welch, B. J., 1992. Adsorption of Hydrogen Fluoride on Alumina. Surface And Interface Analysis, 19, 139-144

[10] Muhammad Javed Iqbal and Muhammad Naseem Ashiq., 2010. Thermodynamics and kinetics of Adsorption of Dyes from Aqueous Media onto Alumina. Journal of Chemical Society of Pakisthan, 32 (4), 419-428

[11] Sushmita Banerjee, Ravindra Kumar Gautam, Amita Jaiswal, Mahesh Chandra Chattopadhyayaa and Yogesh Chandra Sharma., 2015. Rapid scavenging of methylene blue dye from aliquid phase by adsorption on aluminananoparticles. RSC Advances, 5 14425-14440. http://dx.doi.org/10.1039/c4ra12235f

[12] Bushra Ismail, Syed Tajammul Hussain, Sohaib Akram., 2013. Adsorption of methylene blue onto spinel magnesium aluminate nanoparticles: Adsorption isotherms, kinetic and thermodynamic studies. Chemical Engineering Journal, 219 395–402. http://dx.doi.org/10.1016/j.cej.2013.01.034

[13] Pranay A Raut, Monal Dutta, Sonali Sengupta, Jayanta Kumar Basu., 2013. Alumina-carbon composite as an effective adsorbent for removal of Methylene Blue and Alizarin Red-s from aqueous solution. Indian Journal Of Chemical Technology, 20, 15-20

[14] Hameed, B, H., Mahmoud, D, K., Ahmad, A, L., 2008. Equilibrium modeling and kinetic studies on the adsorption of basic dye by a low-cost adsorbent: Coconut (*Cocosnucifera*) bunch waste. Journal of Hazardous Materials, 158, 65–72. http://dx.doi.org/10.1016/j.jhazmat.2008.01.034

[15] Mohd. Rafatullah., Othman Sulaiman., Rokiah Hashim., Anees Ahmad., 2010. Adsorption of methylene blue on low-cost adsorbents: A Review. Journal of Hazardous Materials, 177, 70-80. http://dx.doi.org/10.1016/j.jhazmat.2009.12.047

[16] Martinsen, A., Skjak-Bræk. G., Smidsrød, O., 1989. Alginate as Immobilization Material: I. Correlation between chemical and physical properties of Alginate Gel Beads. Biotechnology and Bioengineering, 33, 79-89.

[17] Assia Benhouria, MdAzharul Islam, H. Zaghouane-Boudiaf, M. Boutahala, B.H.Hameed, 2.15. Calcium alginate-bentonite-activated carbon composite beads as highly effective adsorbent for methylene blue. Chemical Engineering Journal, 270, 621-630. http://dx.doi.org/10.1016/j.cej.2015.02.030

[18] Apel, M. L., Torma A. E., 1993. Determination of Kinetics and Diffusion Coefficients of Metal Sorption on Ca-alginate beads. The Canadian Journal of Chemical Engineering, 71, 652-656

[19] Rathinam Aravindhan, Nishtar Nishad Fathima, Jonnalagadda Raghava Roa, Balachandran Unni Nair., 2007. Equilibrium and thermodynamic studies on the removal of basic black dye using calcium alginate beads. Colloids and Surfaces A: physicochem. Eng. Aspects, 299 232-238.http://dx.doi.org/10.1016/j.colsurfa.2006.11.045

[20] Hassan, A, F., Abdel-Mohsen Moustafa, M,G., 2014. Comparative study of calcium alginate, activated carbon, and their composite beads on methylene blue adsorption. Carbohydrate Polymers, 102, 192-198. http://dx.doi.org/10.1016/j.carbpol.2013.10104

[21] Vincent Rocher, Jean-Michel Siaugue, Valerie Cabuil, Agnes Bee., 2008. Removal of organic dyes by magnetic alginate beads. Water Research 42, 1290-1298. http://dx.doi.org/10.1016/j.watres.2007.09.024

[22]Yanhui Li, Qiuju Du, Tonghao Liu, Jiankun Sun, Yonghao Wang, Shaoling Wu, Zonghua Wang, Yanzhi Xia, Linhua Xia., 2013. Methylene blue adsorption on graphene oxide/calcium alginate composites. Carbohydrate Polymers, 95 (1), 501–507. http://dx.doi.org/10.1016/j.carbpol.2013.01.094

[23] Monika Jain, Garg, V, K., Kadirvelu, K., 2013. Cadmium(II) sorption and desorption in a fixed bed column using sunflower waste carbon calcium–alginate beads.Biosource Technology, 129, 242–248. http://dx.doi.org/10.1016/j.biortech.2012.11.036

[24] Foo,K,Y., Hameed, B, H., 2010. Insights into the modeling of adsorption isotherm systems. Chemical Engineering Journal, 156, 2-10. http://dx.doi.org/10.1016/j.cej.2009.09.013

[25] Hong Zheng, Donghong Liu, YanZheng, Shuping Liang, Zhe Liu., 2009. Sorption isotherm and kinetic modelling of aniline on Cr-bentonite. Journal of Hazardous Materials, 167, 141-147.http://dx.doi.org/10.1016/j.jhazmat.2008.12.093

[26] Bujadak, J., and Komadel, P., 1997. Interaction of methylene blue with reduced charge montmorillonite. Journal of Physical Chemistry B, 101 9065-9068

[27] Maecelo, J. Avena, Laura, E. Valenti, Valeria Pfaffen., Carlos, P. De Pauli., 2001. Methylene blue dimerization does not interfere in surface area measurements of Kaolinite and Soils, Clays and Clay Minerals, 49 (2), 168-173. http://dx.doi.org/10.1346/CCMN.2001.0490206

[28] Giles, C. H., McEwan, J. H., Nakhwa, S.N., and Smith, D., 1960. Studies in Adsorption. Part XI. A system of classification of solution adsorption isotherms and its use in diagnosis of adsorption mechanisms and in measurements of specific areas of soils. Journal of the Chemical Society (Resumed), 3973-3993. http://dx.doi.org/10.1039/JR9600003973

[29] Voytusky, S., 1978. Colloid Chemistry, Mir Publishers, Moscow, pp-212.

[30] Jingfeng Gao, Qian Zhang, Kai Su, Ranni Chen, Yongzhen Peng., 2010. Biosorption of Acid Yellow 17 from aqueous solution by non-living aerobic granular sludge. Journal of Hazardous Materials, 174, 215-225.http://dx.doi.org/10.1016/j.jhazmat.2009.09.039

[31] Christian Taty-Costodes V, Henri Fauduet, Catherine Porte, Yuh-Shan Ho., 2005. Removal of lead (II) ions from synthetic and real effluents using immobilized Pinussylvestrissawdust: Adsorption on a fixed-bed column. Journal of Hazardous Materials B123, 135–144 http://dx.doi.org/10.1016/j.jhazmat.2005.03.032

[32] Emine Malkoc, Yasar Nuhoglu., 2006. Removal of Ni(II) ions from aqueous solutions using waste of tea factory: Adsorption on a fixed-bed column. Journal of Hazardous Materials B135, 328–336 http://dx.doi.org/10.1016/j.jhazmat.2005.11.070

[33] Jyotsna Goel, Krishna Kadirvelu,Chitra Rajagopal, Vinod Kumar Garg., 2005. Removal of lead(II) by adsorption using treated granular activated carbon: Batch and column studies. Journal of Hazardous Materials B125, 211-220. http://dx.doi.org/10.1016/j.jhazmat.2005.05.032

[34] Runping Han, Yu Wang, Xin Zhao, Yuanfeng Wang, Fuling Xie, Junmei Cheng, Mingsheng Tang., 2009. Adsorption of methylene blue by phoenix tree leaf powder in a fixed-bed column: experiments and prediction of breakthrough curves. Desalination 245, 284-297. http://dx.doi.org/10.1016/j.desal.2008.07.013